

## Comparative Study of Cells and Microcircuits in the Rodent and Human Brain (D1.6.3 - SGA2)

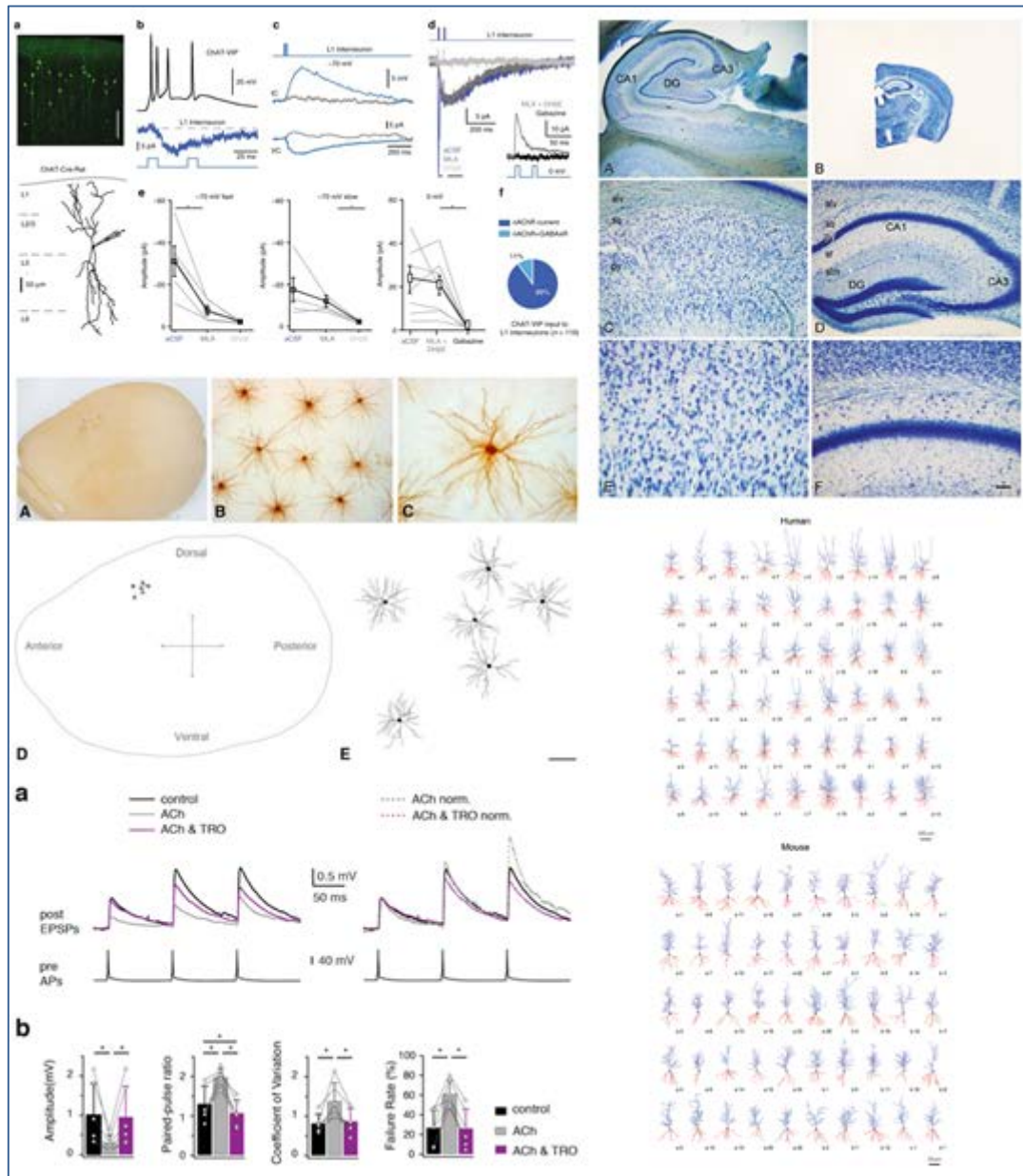


Figure 1: Examples of SP1 Outputs contributing to the comparative studies across species

<b>Project Number:</b>	785907	<b>Project Title:</b>	Human Brain Project SGA2
<b>Document Title:</b>	Comparative Study of Cells and Microcircuits in the Rodent and Human Brain		
<b>Document Filename:</b>	D1.6.3 (D7.3 D35) SGA2 M24 ACCEPTED 201005.docx		
<b>Deliverable Number:</b>	SGA2 D1.6.3 (D7.3, D35)		
<b>Deliverable Type:</b>	Report		
<b>Work Packages:</b>	WP1.5 with contributions from WP1.1 and WP1.4		
<b>Key Result(s):</b>	KR1.2, KR1.4, KR1.5		
<b>Dissemination Level:</b>	PU		
<b>Planned Delivery Date:</b>	SGA2 M24 / / 31 Mar 2020		
<b>Actual Delivery Date:</b>	SGA2 M26 / 26 May 2020 ; resubmitted 9 Sep 2020 and 1 Oct 2020; accepted 5 Oct 2020		
<b>Author(s):</b>	Javier DEFELIPE, UPM (P67), Pilar F. ROMERO, UPM (P68)		
<b>Compiled by:</b>	Pilar F. ROMERO, UPM (P68)		
<b>Contributor(s):</b>	Huib MANSVELDER, VU (P113) Chapters 1-4 Javier DEFELIPE, UPM (P68), Chapters 1-4 Ángel MERCHÁN, UPM (P68), Chapter 3 Lidia ALONSO, UPM (P68), Chapter 3 Ruth BENAVIDES-PICCIONE, UPM (P68), Chapter 3 Pilar F. ROMERO, UPM (P68), Chapters 1-4 Francisco CLASCA, UAM (P64), Chapter 3 Concha BIELZA, UPM (P68), Chapter 3 Bojan MIHALJEVIC, UPM (P68), Chapter 3 Pedro LARRAÑAGA, UPM (P68) Chapter 3 Luis PASTOR, URJC (P69), Chapter 3 María GARCÍA-AMADO, UAM (P64) Chapter 3 Alberto MUÑOZ, UPM (P68) Chapter 3 Silvia TAPIA, UPM (P68) Chapter 3 Dirk FELDMEYER, JUELICH (P20) Chapter 3		
<b>SciTechCoord Review:</b>	Martin TELEFONT, EPFL (P1)		
<b>Editorial Review:</b>	Annemieke MICHELS, EPFL (P1)		
<b>Description in GA:</b>	Report on the final comparative study of cells and microcircuits in the rodent and human brain.		
<b>Abstract:</b>	This report outlines the comparative studies performed in SP1 by using high-level quality data generated in this SP during the SGA2. A total of 7 Outputs are described including (i) publications addressing comparative studies, (ii) main contributions (in terms of data) to implement comparative studies, and (iii) new statistical methods to carry out machine learning-based comparative studies of the microanatomy and		

	physiology of both rodent and human brain. The validation and use of these outputs, as well as their significance within and outside the HBP, are also outlined.
<b>Keywords:</b>	Comparative studies, anatomical data, physiological data, differences, similarities, mouse, rat, human
<b>Target Users/Readers:</b>	Consortium members, Neuroscience community, Computational neuroscience community.

## Table of Contents

1. Overview .....	5
2. Introduction .....	6
3. Key Result KR1.5 Strategic datasets on single neurons and circuits to be used in comparative studies on human and rodent .....	7
3.1 Outputs .....	7
3.1.1 Overview of Outputs .....	7
3.1.2 Output 1: Lateral inhibition by Martinotti interneurons is facilitated by cholinergic inputs in human and mouse neocortex .....	8
3.1.3 Output 2: Group I mGluR-Mediated Activation of Martinotti Cells Inhibits Local Cortical Circuitry in Human Cortex .....	9
3.1.4 Output 3: Prefrontal cortical ChAT-VIP interneurons provide local excitation by cholinergic synaptic transmission and control attention .....	11
3.1.5 Output 4: Differential structure of hippocampal CA1 pyramidal neurons in the human and mouse .....	13
3.1.6 Output 5: Differential expression of secretagogin immunostaining in the hippocampal formation and the entorhinal and perirhinal cortices of humans, rats, and mice .....	15
3.1.7 Output 6: Calbindin immunostaining in the CA1 hippocampal pyramidal cell layer of the human and mouse: A comparative study .....	17
3.1.8 Output 7: Cell Type-Specific Modulation of Layer 6A Excitatory Microcircuits by Acetylcholine in Rat Barrel Cortex .....	19
3.1.9 Output 8: Comparing basal dendrite branches in human and mouse hippocampal CA1 pyramidal neurons with Bayesian networks .....	20
3.1.10 Others .....	22
3.2 Validation and Impact .....	23
3.2.1 Actual and Potential Use of Output(s) .....	23
3.2.2 Publications .....	25
4. Conclusion and Outlook .....	26
5. Annex 1: SP1 Components .....	27

## Table of Tables

Table 1: Output 1 Links .....	8
Table 2: Output 2 Links .....	11
Table 3: Output 3 Links .....	13
Table 4: Output 4 Links .....	15
Table 5: Output 5 Links .....	17
Table 6: Output 6 Links .....	18
Table 7: Output 7 Links .....	19
Table 8: Output 8 Links .....	22

## Table of Figures

Figure 1: Examples of SP1 Outputs contributing to the comparative studies across species .....	1
Figure 2: Cholinergic inputs depolarize Martinotti cells .....	9
Figure 3: ' <i>mGluR activation increases synaptic inhibition onto human pyramidal neurons</i> '. .....	10
Figure 4: ' <i>Direct synaptic inputs to L6 pyramidal neurons</i> ' .....	12
Figure 5: ' <i>Confocal microscopy images of human neurons injected with LY in the hippocampus</i> ' .....	14
Figure 6: ' <i>Confocal microscopy images of mouse neurons injected with LY in the hippocampus</i> ' .....	14
Figure 7: ' <i>Comparison of the patterns of SCGN-immunoreactivity in the hippocampus of the rat and mouse</i> ' .....	16
Figure 8: ' <i>CB-ir neurons show sub-laminar distribution in mouse CA1 pyramidal cell layer</i> ' .....	18
Figure 9: ' <i>ACh hyperpolarizes CC L6A PCs but depolarizes CT L6A PCs</i> ' .....	20
Figure 10: ' <i>Bayesian networks learned from the terminal branches</i> ' .....	21

### History of Changes made to this Deliverable (post Submission)

Date	Change Requested / Change Made / Other Action
25 May 2020	Deliverable submitted to EC
06 Aug 2020	Resubmission with specified changes requested in Review Report Main changes requested: <ul style="list-style-type: none"> <li>• Change 1: References to components need to be added (extract from Review Report)</li> <li>• Change 2: References to WPs, tasks and Outputs need to be added (extract from Review Report)</li> <li>• Change 3: ToC containing almost only numbers (extract from Review Report)</li> </ul>
11 Aug 2020	Revised draft sent by SP/CDP to PCO. Main changes made, with indication where each change was made: <ul style="list-style-type: none"> <li>• Change 1: References to components included in a new annex (see Annex 1: SP1 Components)</li> <li>• Change 2: References to WPs, Tasks and Outputs added (see Sections 1-4)</li> <li>• Change 3: ToC updated - headers are now descriptive</li> <li>• Change 4: some provisional links were replaced by final public KG links (Section 3.1)</li> </ul>
4 Sep 2020	Editorial proofreading
9 Sep 2020	Revised version resubmitted to EC by PCO via SyGMA
1 Oct 2020	Minor editorial change by PCO
1 Oct 2020	Revised version resubmitted to EC by PCO via SyGMA

# 1. Overview

The human brain shares many common features with other nonhuman mammals that might be considered as basic bricks of brain organisation, which –by definition– are common to all mammalian species. Therefore, choosing appropriate experiments to obtain strategic data that could be extrapolated to the human brain is a major goal in neuroscience. For this general purpose, many neuroscientists suggest that the ideal experimental animals at present are rodents because they can be manipulated to study many aspects from genes to behaviour. Furthermore, we can use relatively large numbers of animals at a relatively low cost.

SP1 Objective SO1.5 ‘Obtaining critical information about differences and similarities in brain organisation across species’, aims to work towards this goal through KR1.5: *Key datasets on single neurons and circuits to be used in comparative studies on human and rodent for modelling. Ground-breaking techniques will be used to generate anatomical and functional datasets. New statistical models will be developed to perform comparative analysis.* The Outputs of this KR include multiple datasets based on rodent and human brain neurons and circuits that have been used to carry out the comparative studies. Furthermore, novel methodologies for multivariate comparison and analysis of anatomical and functional data have been developed to implement comparative studies.

Finally, the strategic comparative data displayed in this Deliverable are being fed directly into theory and model simulations in SP4 (Theoretical Neuroscience) and SP6 (Brain Simulation Platform). Thereby, this KR provides anchor points for translation from rodent neuronal circuit simulations to human neuronal circuit simulations. The data generated in this Deliverable are critical for the transition of the scientific objectives from SGA2 to SGA3, particularly for WP1: *The Human Multiscale Brain Connectome and its Variability* that will be focused on the human brain.

## 2. Introduction

The overarching objective of SP1 is to generate neuroscientific concepts, knowledge, experimental datasets and tools, which will be used to build models for the simulation of the brain. In addition, SP1 will provide data and knowledge to support activities undertaken by other SPs and CDPs (mainly SP6, but also SP4, SP10, Neurorobotics Platform) and CDPs (mainly CDP1 and CDP2).

During the SGA2, SP1 has acquired data mostly on the mouse brain, and to limited degree on the human brain. The work plan has focused on fundamental questions, coordinated at the HBP level, on structural organisation, neuronal activity, microcircuit dynamics, synaptic plasticity and neuromodulation required to fuel and complement modelling and theory. The SP1 studies have adopted all advanced techniques required for SP1 to meet the needs of in particular SP6. This includes performing inter-domain analyses and across-scale investigations encompassing molecular, anatomical and functional data integration in rodents, and carry out comparative studies of cells and microcircuits in the rodent and human brain.

A total of five Key Results (KRs) were planned in SP1 for the SGA2 (KR1.1-KR1.5). The present report outlines the comparative studies carried out in this SP1 to contribute to KR1.5. This KR is intended to meet SP1 Objective SO1.5, which aims to obtain critical information about differences and similarities in brain organisation across species. The comparative studies have been implemented by using datasets generated mainly in WP1.5: *Comparative study of cells and microcircuits in the rodent and human brain*, as well as in other WPs, such as WP1.2: *Cell and Microcircuitry: neocortex, hippocampus, basal ganglia and cerebellum*, to contribute to KR1.5. These datasets have been released and detailed information can be found in SGA2 Deliverables D1.6.1 and D1.6.2.

In this Deliverable, Outputs 1-6 are publications that address comparative studies carried out during SGA2. In addition, Output 7 is described as a main contribution to implement comparative studies. Finally, Output 8 shows an example on how to use data generated in SP1 to develop statistical models. The validation and use of these Outputs, as well as their significance within and outside the HBP, are also outlined.

The scientific excellence of the datasets that have been generated in SP1 and used in the comparative studies is proved by their publication in high-level neuroscience journals.

## 3. Key Result KR1.5 Strategic datasets on single neurons and circuits to be used in comparative studies on human and rodent

### 3.1 Outputs

#### 3.1.1 Overview of Outputs

Main outputs outlined below are SP1 publications that address comparative studies between rodent and humans and have been generated by using the obtained datasets. Statistical models to carry out comparative studies are also included. These publications have been generated by using the high-level datasets generated mainly in WP1.5: *Comparative study of cells and microcircuits in the rodent and human brain* according to the SP1 Data Plan. Most of these Outputs are publications resulting from collaborations between several SPs. These comparative studies across species are planned as part of Key Result KR1.5: *Key datasets on single neurons and circuits to be used in comparative studies on human and rodent for modelling. Ground-breaking techniques will be used to generate anatomical and functional datasets. New statistical models will be developed to perform comparative analysis to achieve SP1 Objective SO1.5: Obtaining critical information about differences and similarities in brain organisation across species*

##### 3.1.1.1 List of Outputs contributing to this KR

- Output 1: Lateral inhibition by Martinotti interneurons is facilitated by cholinergic inputs in human and mouse neocortex (P1410; C1729, C1730, C1731)
- Output 2: Group I mGluR-Mediated Activation of Martinotti Cells Inhibits Local Cortical Circuitry in Human Cortex (P1962; C1729, C1730, C1731)
- Output 3: Prefrontal cortical ChAT-VIP interneurons provide local excitation by cholinergic synaptic transmission and control attention (P2212; C1729, C1730, C1731)
- Output 4: Differential structure of hippocampal CA1 pyramidal neurons in the human and mouse (P1963; C1740, C1741)
- Output 5: Differential expression of secretagogin immunostaining in the hippocampal formation and the entorhinal and perirhinal cortices of humans, rats, and mice (P2147; C1740, C1741)
- Output 6: Calbindin immunostaining in the CA1 hippocampal pyramidal cell layer of the human and mouse: A comparative study (P2380; C1740, C1741)
- Output 7: Cell Type-Specific Modulation of Layer 6A Excitatory Microcircuits by Acetylcholine in Rat Barrel Cortex (P2118; C2345)
- Output 8: Comparing basal dendrite branches in human and mouse hippocampal CA1 pyramidal neurons with Bayesian networks (P2428, P1722, P1723, P1724, P1821, P2138; C1740, C1802).

The Components contributing to this Deliverable can be found in Annex 1: SP1 Components.

##### 3.1.1.2 How Outputs relate to each other and the Key Result

Outputs described in this Deliverable relate to each other and to KR1.5 by implementing comparative studies across species using strategic datasets on single neurons and circuits and new statistical models generated in SP1 to accomplish this KR. These Outputs have been generated to meet SP1 Objective SO1.5.

### 3.1.2 *Output 1: Lateral inhibition by Martinotti interneurons is facilitated by cholinergic inputs in human and mouse neocortex*

Data released of Components C1729, C1730, and C1731 (T1.5.2: Comparative physiology of mouse and human neocortical excitatory synapses, T1.5.3: Comparative physiology of mouse and human neocortical pyramidal neurons and interneurons in different layers and T1.5.4: Comparative physiology of neuromodulation of neocortical circuits in mouse and human brain) have contributed to this publication.

**Publication abstract:** *'A variety of inhibitory pathways encompassing different interneuron types shape activity of neocortical pyramidal neurons. While basket cells (BCs) mediate fast lateral inhibition between pyramidal neurons, Somatostatin-positive Martinotti cells (MCs) mediate a delayed form of lateral inhibition. Neocortical circuits are under control of acetylcholine, which is crucial for cortical function and cognition. Acetylcholine modulates MC firing, however, precisely how cholinergic inputs affect cortical lateral inhibition is not known. Here, we find that cholinergic inputs selectively augment and speed up lateral inhibition between pyramidal neurons mediated by MCs, but not by BCs. Optogenetically activated cholinergic inputs depolarize MCs through activation of  $\beta_2$  subunit-containing nicotinic AChRs, not muscarinic AChRs, without affecting glutamatergic inputs to MCs. We find that these mechanisms are conserved in human neocortex. Cholinergic inputs thus enable cortical pyramidal neurons to recruit more MCs, and can thereby dynamically highlight specific circuit motifs, favouring MC-mediated pathways over BC-mediated pathways.'*

*'Main highlights:*

- *Delayed lateral inhibition is selectively enhanced by basal forebrain cholinergic inputs*
- *Cholinergic inputs directly depolarize MCs*
- *ACh does not affect synaptic strength between pyramidal and MCs*
- *Cholinergic inputs advance and prolong MC action potential (AP) firing*
- *Lateral inhibition in human temporal cortex*
- *Acetylcholine enhances lateral inhibition by activating nAChRs in human temporal cortex*
- *ACh depolarizes human putative Martinotti cells and alters AP firing properties'*

**Table 1: Output 1 Links**

Component	Link to	URL
C1729, C1730, C1731	Data Repository	<a href="https://www.nature.com/articles/s41467-018-06628-w#Ack1">https://www.nature.com/articles/s41467-018-06628-w#Ack1</a>
	Technical and user documentation	<a href="https://www.nature.com/articles/s41467-018-06628-w#Ack1">https://www.nature.com/articles/s41467-018-06628-w#Ack1</a>

SPs involved: SP1- Mouse Brain Organization and Interspecies Comparisons and SP2 Human Brain Organization.

Publication reference:

P1410: Lateral inhibition by Martinotti interneurons is facilitated by cholinergic inputs in human and mouse neocortex. Obermayer J, Heistek TS, Kerkhofs A, Goriounova NA, Kroon T, Baayen JC, Idema S, Testa-Silva G, Couey JJ, Mansvelter HD. 5 October 2018. DOI: 10.1038/s41467-018-06628-w.

Documentation, materials, analysis scripts and raw data can be provided upon request from the corresponding author

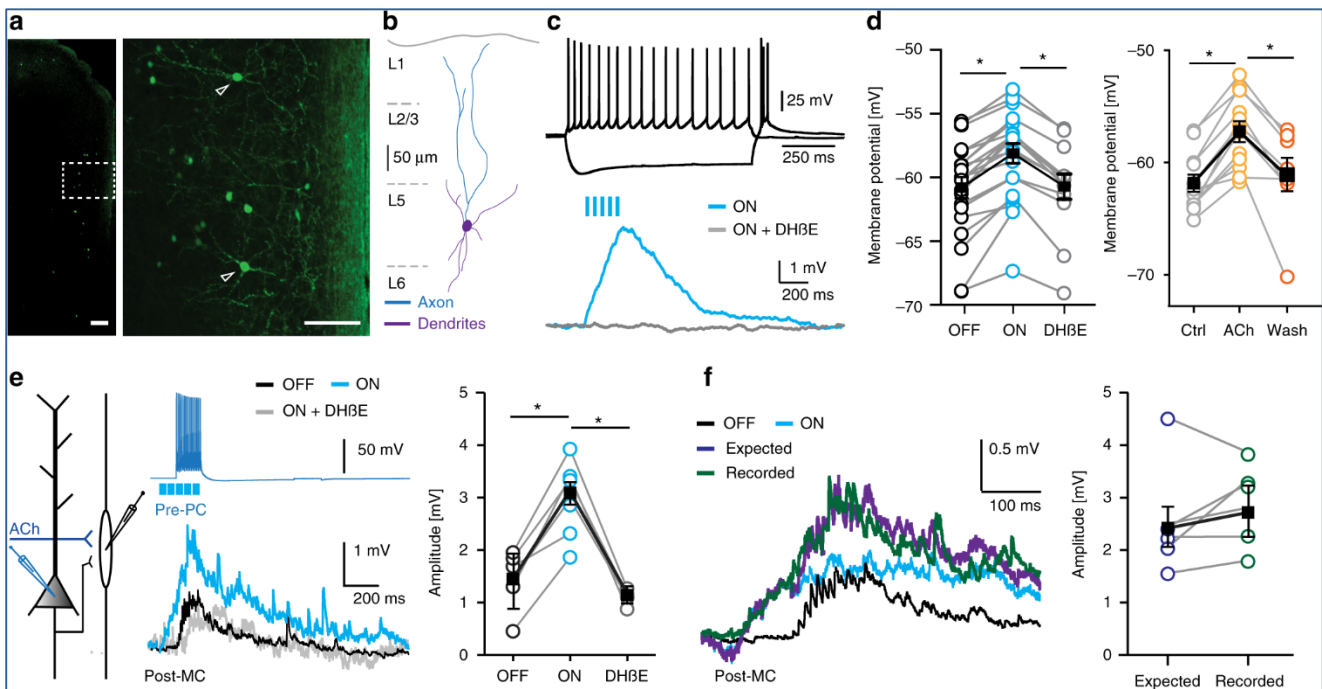


Figure 2: Cholinergic inputs depolarize Martinotti cells

A GFP-labelled SOM + interneurons in a GIN mouse (scale bar 200  $\mu$ m). b Digital reconstruction of a GFP-expressing MC. c Top trace: Action potential profile of a L5 MC in a GIN/Chat-ChR2-EYFP mouse in response to somatic current injection (+100 pA and -150 pA). Bottom trace: Example trace (Blue trace) of a nAChR-mediated response in a L5 MC in the mPFC. The postsynaptic response was blocked by DHBE (10  $\mu$ M, gray trace). d Left: Summary chart showing the maximum amplitude of nAChR-EPSPs in L5 MCs in the mPFC evoked by optogenetic triggered ACb release (light OFF  $-60.68 \pm 0.82$  mV, light ON  $-58.00 \pm 0.76$  mV, DHBE  $-60.60 \pm 1.00$  mV,  $F(2, 52) = 3.488$ , one-way ANOVA,  $p = 0.038$ ,  $n = 23$ ; mean  $\pm$  s.e.m.). Right: Summary chart indicating the depolarization of L2/3 MCs of S1 by application of ACh (1 mM) (Ctrl.  $-61.8 \pm 0.75$  mV, ACh  $-57.2 \pm 0.94$  mV, wash  $-61.0 \pm 1.48$  mV, paired t-test, two-tailed,  $p = 0.0005$ ,  $t = 8.288$ ,  $df = 11$ ,  $n = 12$ ). e Right: Setup of the experiment. Middle: Example traces of synaptically connected pre-PC and postsynaptic MC (Post-MC). Middle top: Pre-PC fired a train of 15 APs at 100 Hz. Optogenetic ACh release was induced by five light pulses at 25 Hz starting 100 ms preceding the first AP. Middle bottom: Postsynaptic responses recorded in a mPFC L5 Post-MC in absence (Black trace) or presence of optogenetic triggered ACh release (Blue trace). The potentiation that is induced by ACh is blocked by DHBE (Gray trace). Right: Summary plot. The combination of glutamatergic EPSPs from the PC and cholinergic excitatory input leads depolarizes the membrane potential (light OFF  $1.54 \pm$  s.e.m. mV, light ON  $3.30 \pm$  s.e.m. mV). This is blocked by application of DHBE (1.07 mV, One-way ANOVA  $F(2, 13) = 16.81$ ,  $p = 0.0002$ ,  $n = 6$ ). f Left: Example trace of a glutamatergic EPSP (Black trace) and nAChR-mediated (Blue trace) EPSPs. The co-occurring of glutamatergic and cholinergic EPSPs (Green trace) leads to larger depolarization. Right: summation of single glutamatergic and nAChR-mediated EPSPs (Expected value, Purple trace,  $2.54 \text{ mV} \pm$  s.e.m.) did not differ from the recorded combined EPSP ( $2.88 \text{ mV} \pm$  s.e.m.,  $p = 0.2766$ , paired t-test, two-tailed,  $t = 1.221$ ,  $df = 5$ ,  $n = 6$ ; mean  $\pm$  s.e.m.)

Source: <https://www.nature.com/articles/s41467-018-06628-w#Ack1> :

Title: publication title

Publication abstract: taken from the publication

Main highlights: taken from the section 'Results' of publication

Figure: example of one figure displayed in the publication

### 3.1.3 Output 2: Group I mGluR-Mediated Activation of Martinotti Cells Inhibits Local Cortical Circuitry in Human Cortex

Data released of Components C1729, C1730, and C1731 (T1.5.2: Comparative physiology of mouse and human neocortical excitatory synapses, T1.5.3: Comparative physiology of mouse and human neocortical pyramidal neurons and interneurons in different layers and T1.5.4: Comparative physiology of neuromodulation of neocortical circuits in mouse and human brain) have contributed to this publication.

Publication abstract: 'Group I metabotropic glutamate receptors (mGluRs) mediate a range of signaling and plasticity processes in the brain and are of growing importance as potential

therapeutic targets in clinical trials for neuropsychiatric and neurodevelopmental disorders (NDDs). Fundamental knowledge regarding the functional effects of mGluRs upon pyramidal neurons and interneurons is derived largely from rodent brain, and their effects upon human neurons are predominantly untested. We therefore addressed how group I mGluRs affect microcircuits in human neocortex. We show that activation of group I mGluRs elicits action potential firing in Martinotti cells, which leads to increased synaptic inhibition onto neighboring neurons. Some other interneurons, including fast-spiking interneurons, are depolarized but do not fire action potentials in response to group I mGluR activation. Furthermore, we confirm the existence of group I mGluR-mediated depression of excitatory synapses in human pyramidal neurons. We propose that the strong increase in inhibition and depression of excitatory synapses onto layer 2/3 pyramidal neurons upon group I mGluR activation likely results in a shift in the balance between excitation and inhibition in the human cortical network’.

‘Main highlights:

- Group I mGluR activation increases inhibition onto human pyramidal neurons
- Group I mGluRs strongly activate Martinotti Cells in human cortex
- Synaptic inhibition onto layer 1 interneurons is increased by group I mGluR activation
- Group I mglurs depolarize fast-spiking interneurons, but do not elicit action potential firing
- Excitatory inputs onto human pyramidal neurons exhibit mglur-mediated depression’

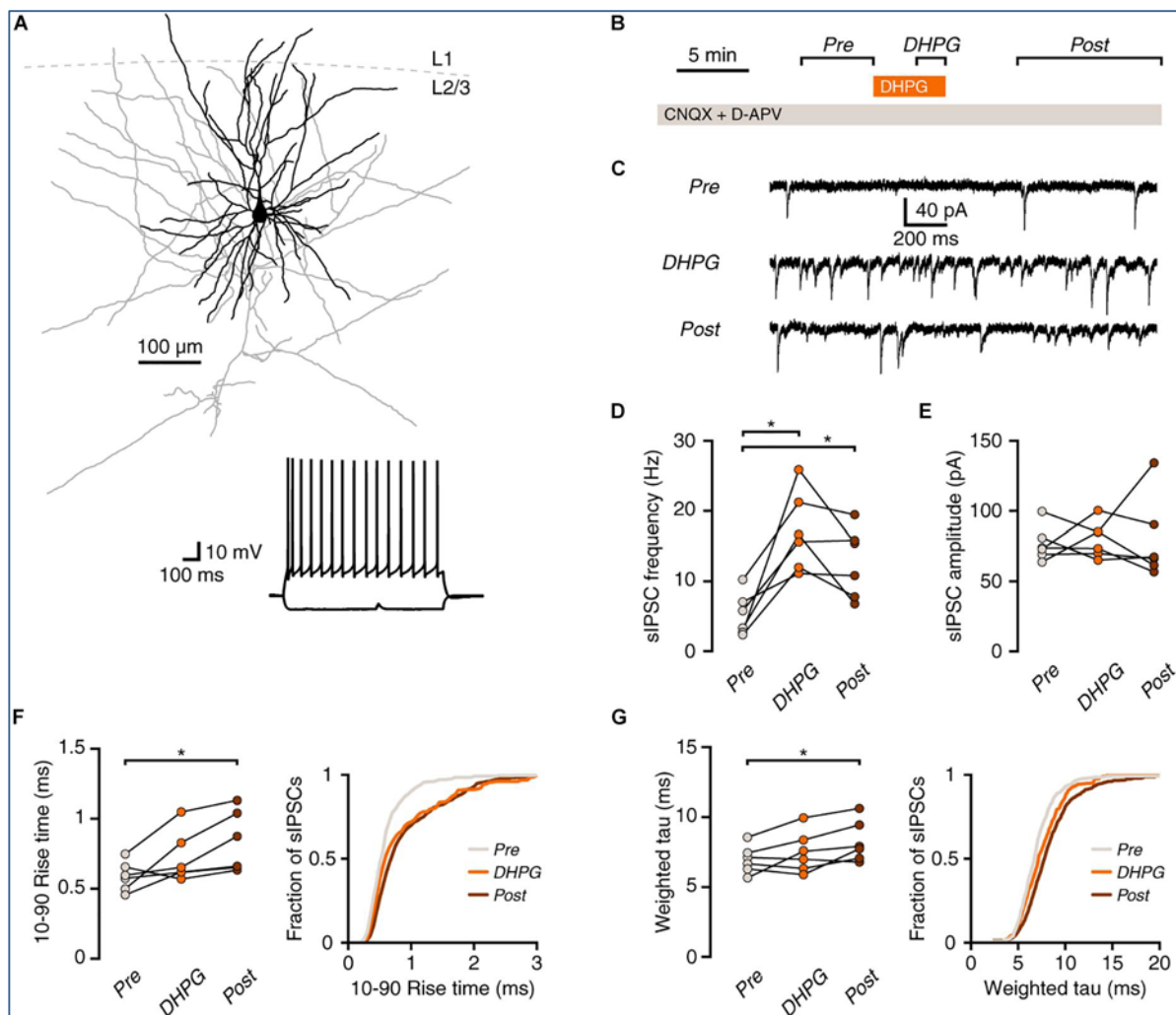


Figure 3: ‘mGluR activation increases synaptic inhibition onto human pyramidal neurons’.

(A) Example morphological reconstruction of a human pyramidal neuron (350  $\mu\text{m}$  slice; dendrites in black, axon in grey). Inset: electrophysiological response to negative and positive current steps. (B) Experimental protocol. (C) Example traces showing IPSCs before (Pre), during (DHPG) and after (Post) application of DHPG. (D) DHPG elicited a lasting increase in sIPSC frequency in pyramidal neurons (repeated-measures ANOVA:  $F(2, 10) = 16.84$ ,  $p = 0.003$ ; Tukey’s post hoc test: Pre vs. DHPG  $*p < 0.05$ , DHPG vs. Post ns, Pre vs. Post  $*p <$

0.05). (E) sIPSC amplitude was not significantly affected by DHPG [ $F(2, 10) = 0.07, p = 0.929$ ]. (F) Average rise time of sIPSCs in pyramidal neurons was slower after DHPG application [ $F(2, 10) = 7.22, p = 0.011$ ; Tukey's post hoc test: Pre vs. DHPG ns, DHPG vs. Post ns, Pre vs. Post \* $p < 0.05$ ]. Right panel, cumulative probability distribution of sIPSC rise times, average of probability distributions calculated for each cell. (G) Decay time of sIPSCs was slower after DHPG application [ $F(2, 10) = 5.82, p = 0.021$ ; Tukey's post hoc test: Pre vs. DHPG ns, DHPG vs. Post ns, Pre vs. Post \* $p < 0.05$ ]. Right panel, cumulative probability distribution of sIPSC decay times, average of probability distributions calculated for each cell

Source: <http://dx.doi.org/10.3389/fncel.2019.00315>:

Title: publication title

Publication abstract: taken from the publication

Main highlights: taken from the section 'Results' of publication

Figure: example of figure displayed in the publication

Table 2: Output 2 Links

Component	Link to	URL
C1729, C1730, C1731	Data Repository	<a href="http://dx.doi.org/10.3389/fncel.2019.00315">http://dx.doi.org/10.3389/fncel.2019.00315</a>
	Technical and user documentation	<a href="http://dx.doi.org/10.3389/fncel.2019.00315">http://dx.doi.org/10.3389/fncel.2019.00315</a>

SPs involved: SPs involved: SP1- Mouse Brain Organization and Interspecies Comparisons and SP2 Human Brain Organization.

Publication reference:

P1962: Group I mGluR-Mediated Activation of Martinotti Cells Inhibits Local Cortical Circuitry in Human Cortex. Kroon T, Dawitz J, Kramvis I, Anink J, Obermayer J, Verhoog MB, Wilbers R, Goriounova NA, Idema S, Baayen JC, Aronica E, Mansvelder HD, Meredith RM. (2019). *Frontiers Cell Neurosci.* 11 July 2019; 13:315. doi: 10.3389/fncel.2019.00315.

Documentation, materials, analysis scripts and raw data can be provided upon request from the corresponding author

### 3.1.4 Output 3: Prefrontal cortical ChAT-VIP interneurons provide local excitation by cholinergic synaptic transmission and control attention

Data released of Components C1729, C1730, C1731 (T1.5.2: Comparative physiology of mouse and human neocortical excitatory synapses, T1.5.3: Comparative physiology of mouse and human neocortical pyramidal neurons and interneurons in different layers and T1.5.4: Comparative physiology of neuromodulation of neocortical circuits in mouse and human brain) have contributed to this publication.

Publication abstract: '*Neocortical choline acetyltransferase (ChAT)-expressing interneurons are a subclass of vasoactive intestinal peptide (ChAT-VIP) neurons of which circuit and behavioural function are unknown. Here, we show that ChAT-VIP neurons directly excite neighbouring neurons in several layers through fast synaptic transmission of acetylcholine (ACh) in rodent medial prefrontal cortex (mPFC). Both interneurons in layers (L)1-3 as well as pyramidal neurons in L2/3 and L6 receive direct inputs from ChAT-VIP neurons mediated by fast cholinergic transmission. A fraction (10-20%) of postsynaptic neurons that received cholinergic input from ChAT-VIP interneurons also received GABAergic input from these neurons. In contrast to regular VIP interneurons, ChAT-VIP neurons did not disinhibit pyramidal neurons. Finally, we show that activity of these neurons is relevant for behaviour and they control attention behaviour distinctly from basal forebrain ACh inputs. Thus, ChAT-VIP neurons are a local source of cortical ACh that directly excite neurons throughout cortical layers and contribute to attention*

'Main highlights:

- Fast cholinergic synaptic transmission by ChAT-VIP neurons
- Direct excitation, but no disinhibition by ChAT-VIP neurons

- Cholinergic synaptic inputs to L6 pyramidal neurons
- Consequences of co-transmission of ACh and GABA
- ChAT-VIP neurons are required for attention'

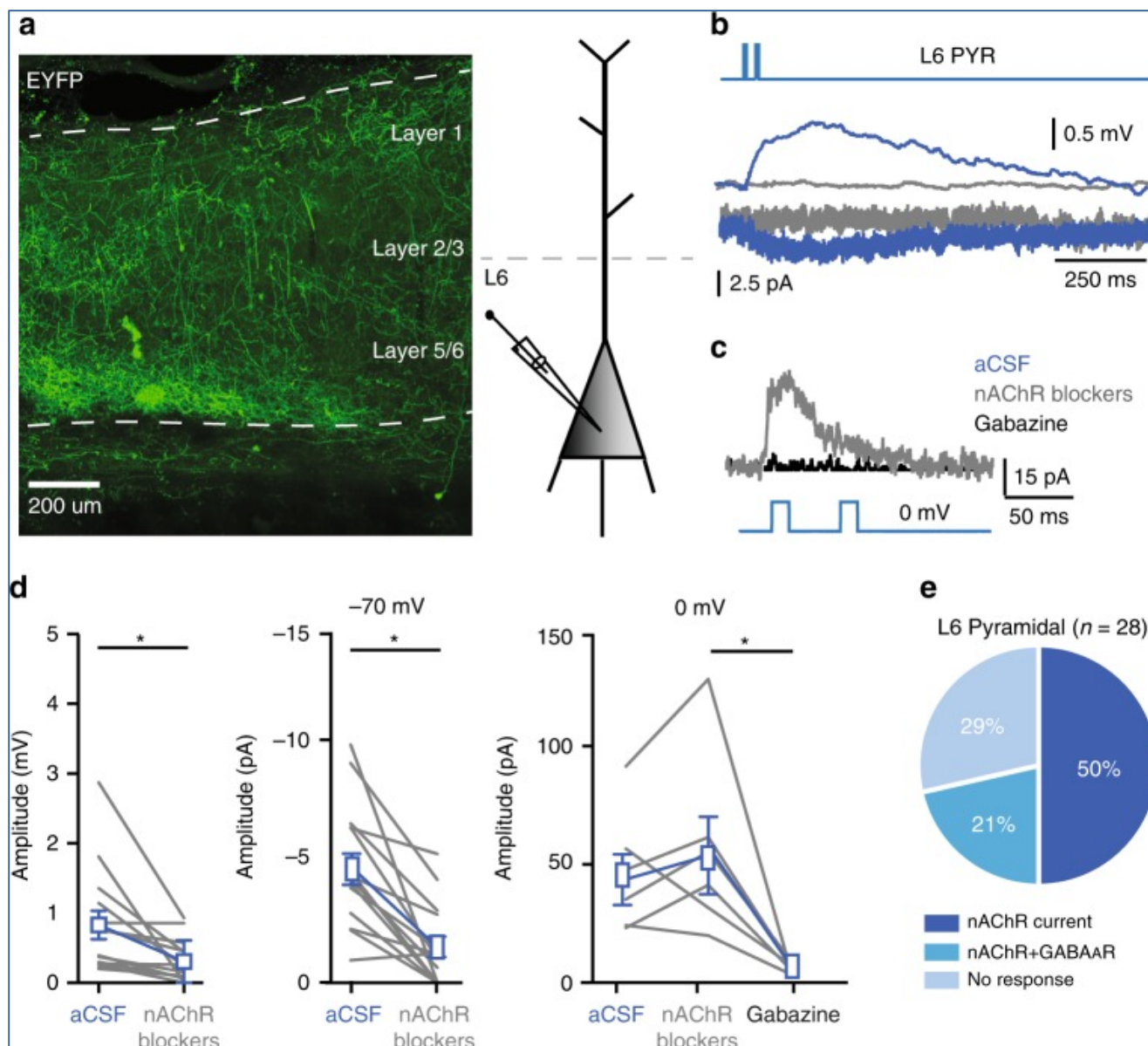


Figure 4: 'Direct synaptic inputs to L6 pyramidal neurons'

'a EYFP expression in ChAT-VIP neurons throughout mPFC layers. Right: schematic illustration of recording set up. b Example traces from a rat L6 pyramidal neuron showing depolarization and an inward current at  $-70$  mV in response to blue-light ChR2-mediated activation of ChAT-VIP neurons (470 nm, 10 ms, 25 Hz) in absence (blue trace) or in the presence of nAChR antagonists (grey trace). c Same L6 pyramidal neuron recorded at 0 mV membrane potential showing light-evoked synaptic current in the presence of nAChR blockers (grey trace) and gabazine (black trace). d Left: summary chart showing the amplitudes of postsynaptic membrane potential changes with and without nAChR blockers. Middle: postsynaptic current amplitudes at  $-70$  mV membrane potential without and with nAChR blockers (aCSF:  $4.820 \pm 0.6853$  pA, nAChR blockers:  $1.483 \pm 0.4594$  pA,  $p = 0.0002$ , paired t-test, two-tailed,  $t = 5.051$ ,  $df = 13$ ;  $n = 14$ , mean  $\pm$  SEM). Right: postsynaptic current amplitudes recorded at 0 mV with nAChR blockers and gabazine (aCSF:  $40.85 \pm 10.35$  pA, nAChR blockers:  $50.65 \pm 15.47$  pA, gabazine:  $1.403 \pm 0.8461$  pA, one-way ANOVA:  $F(5, 10) = 2.949$ ,  $p = 0.0148$ ;  $n = 6$ , mean  $\pm$  SEM). Summary plots show averages  $\pm$  SEM. e Pie chart showing percentages of L6 pyramidal neurons with nAChR-mediated, combined nAChR and GABAAR-mediated, and no synaptic currents'.

Source: <http://dx.doi.org/10.1038/s41467-019-13244-9>

Title: publication title

Publication abstract: taken from the publication

Main highlights: taken from the section 'Results' of publication

Figure: example of one figure displayed in the publication

Table 3: Output 3 Links

Component	Link to	URL
C1729,	Data Repository	<a href="http://dx.doi.org/10.1038/s41467-019-13244-9">http://dx.doi.org/10.1038/s41467-019-13244-9</a>
C1730, C1731	Technical and user documentation	<a href="http://dx.doi.org/10.1038/s41467-019-13244-9">http://dx.doi.org/10.1038/s41467-019-13244-9</a>

Publication reference:

P2212: Prefrontal cortical ChAT-VIP interneurons provide local excitation by cholinergic synaptic transmission and control attention. Obermayer J, Luchicchi A, Heistek TS, de Kloet SF, Terra H, Bruinsma B, Mnie-Filali O, Kortleven C, Galakhova AA, Khalil AJ, Kroon T, Jonker AJ, de Haan R, van de Berg WDJ, Goriounova NA, de Kock CPJ, Pattij T, Mansvellder HD. (2019) Nature Communications. 21 Nov 2019, 10(1): 5280. doi: 10.1038/s41467-019-13244-9.

Documentation, materials, analysis scripts and raw data can be provided upon request from the corresponding author

### 3.1.5 *Output 4: Differential structure of hippocampal CA1 pyramidal neurons in the human and mouse*

Components C1740 and C1741 (T1.5.1: Comparative studies of microanatomy of pyramidal neurons and synaptology in the neocortex and hippocampus of rodents and humans) have contributed to this publication.

Publication abstract: *'Pyramidal neurons are the most common cell type and are considered the main output neuron in most mammalian forebrain structures. In terms of function, differences in the structure of the dendrites of these neurons appear to be crucial in determining how neurons integrate information. To further shed light on the structure of the human pyramidal neurons we investigated the geometry of pyramidal cells in the human and mouse CA1 region—one of the most evolutionary conserved archicortical regions, which is critically involved in the formation, consolidation, and retrieval of memory. We aimed to assess to what extent neurons corresponding to a homologous region in different species have parallel morphologies. Over 100 intracellularly injected and 3D-reconstructed cells across both species revealed that dendritic and axonal morphologies of human cells are not only larger but also have structural differences, when compared to mouse. The results show that human CA1 pyramidal cells are not a stretched version of mouse CA1 cells. These results indicate that there are some morphological parameters of the pyramidal cells that are conserved, whereas others are species-specific'.*

*'Main highlights:*

- *Human CA1 pyramidal neurons exhibit distinctive morphological complexity, which bears important computational implications*
- *Human CA1 cells are not only larger but also have a structurally different organization compared to mouse cells*
- *Some morphological parameters of the CA1 pyramidal cells that are conserved, whereas others are species-specific'*

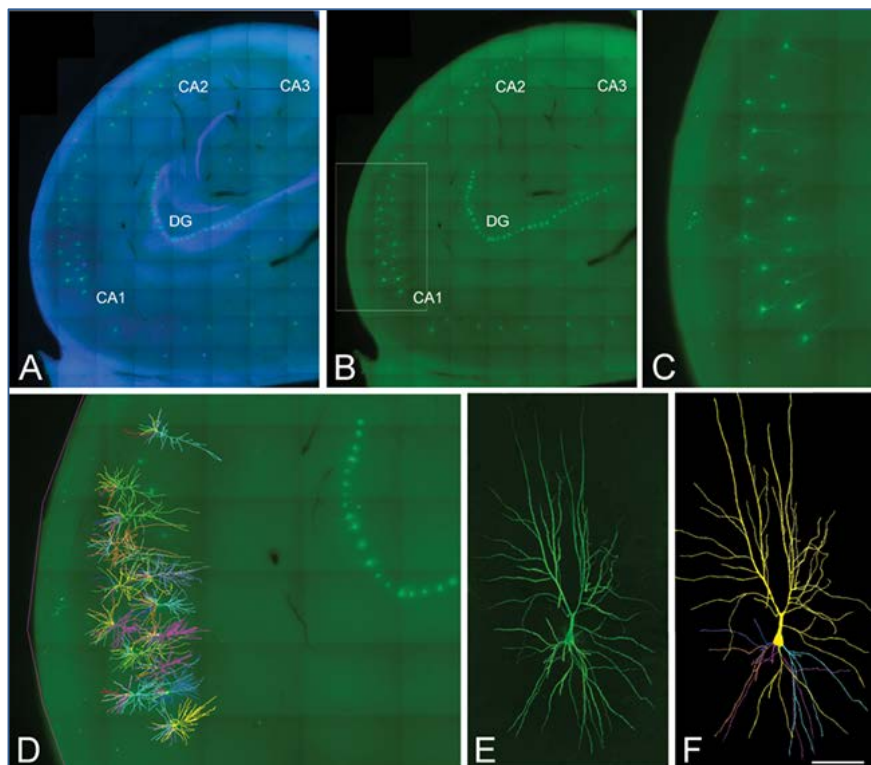


Figure 5: 'Confocal microscopy images of human neurons injected with LY in the hippocampus'

'(A and B) Labeled pyramidal cells (green) and DAPI staining (blue) in different regions of the human hippocampus, including CA1, CA2, CA3, and the dentate gyrus (DG) region. (C) Higher magnification image of the boxed region shown in (B). (D) 3D-reconstructed cells superimposed on the confocal image shown in (C). (E and F) High-magnification image z projection showing an injected CA1 pyramidal cell (E) and the 3D reconstruction of the same cell (F). Scale bar (in panel F) is equal to 1100  $\mu\text{m}$  in (A) and (B); 460  $\mu\text{m}$  in (C) and (D); 100  $\mu\text{m}$  in (E) and (F)'.

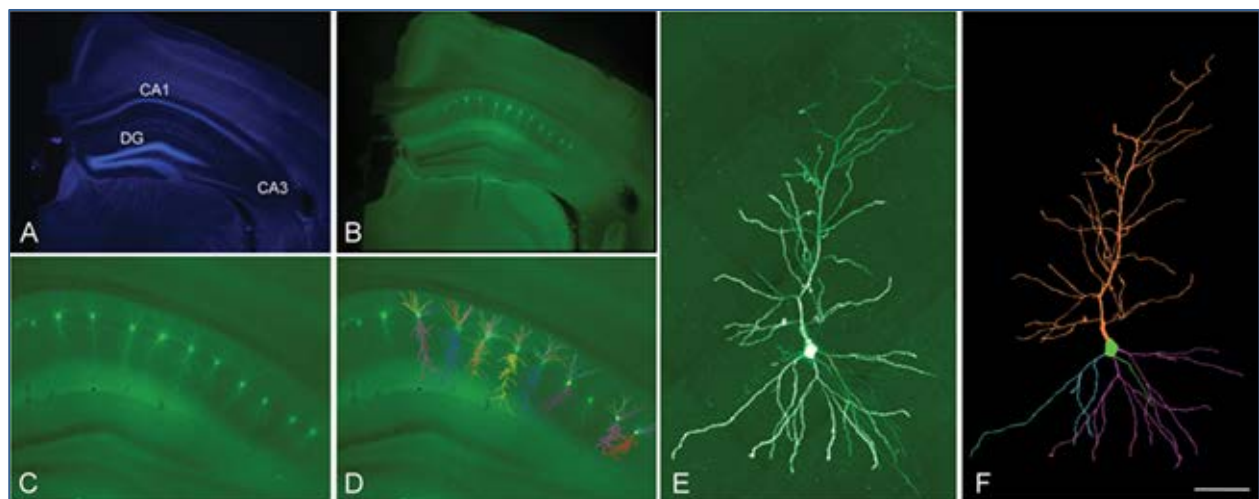


Figure 6: 'Confocal microscopy images of mouse neurons injected with LY in the hippocampus'

'(A) DAPI staining. (B) Labeled pyramidal cells in the CA1 hippocampal field. (C) Higher magnification photomicrographs of the image shown in (B). (D) 3D-reconstructed cells superimposed on the confocal image shown in (C). (E and F) High-magnification image z projection showing an injected CA1 pyramidal cell (E) and the 3D reconstruction of the same cell (F). Scale bar (in panel F) is equal to 750  $\mu\text{m}$  in (A) and (B); 300  $\mu\text{m}$  in (C) and (D); 50  $\mu\text{m}$  in (E) and (F)'.

Source: <https://academic.oup.com/cercor/article/30/2/730/5527134> :

Title: publication title

Publication abstract: taken from the publication

Main highlights: written by the author for this report

Figure: example of two figures displayed in the publication

Table 4: Output 4 Links

Component	Link to	URL
C1740, C1741	Data Repository	C1740: <a href="https://kg.ebrains.eu/search/instances/Dataset/2d3757b5-afc8-470d-988e-f382884cf382">https://kg.ebrains.eu/search/instances/Dataset/2d3757b5-afc8-470d-988e-f382884cf382</a> (embargoed); DOI: <a href="https://doi.org/10.25493/H24F-2ET">10.25493/H24F-2ET</a> C1741: <a href="https://kg.ebrains.eu/search/instances/Dataset/1e87bd86-25fa-43dd-85c6-fc043d4b2687">https://kg.ebrains.eu/search/instances/Dataset/1e87bd86-25fa-43dd-85c6-fc043d4b2687</a> (embargoed); DOI: <a href="https://doi.org/10.25493/PJG9-ZE6">10.25493/PJG9-ZE6</a>
	Technical and User documentation	'Data descriptor' is in the KG (see above links)

SPs involved: SP1 - Mouse Brain Organization and Interspecies Comparisons; SP4 - Theoretical Neuroscience; SP6 - Brain Simulation Platform (T6.2.5 - Human neurons - detailed models from structure to activity)

Publication reference:

P1963: Differential structure of hippocampal CA1 pyramidal neurons in the human and mouse. Benavides-Piccione R, Regalado-Reyes M, Fernaud-Espinosa I, Kastanauskaite A, Tapia-González S, León-Espinosa G, Rojo C, Insausti R, Segev I, DeFelipe J (2019) Cerebral Cortex, 2 July 2019; 00: 1-23. doi: 10.1093/cercor/bhz122.

### 3.1.6 *Output 5: Differential expression of secretagogin immunostaining in the hippocampal formation and the entorhinal and perirhinal cortices of humans, rats, and mice*

Data (images) generated in Components C1740 and C1741 (T1.5.1: Comparative studies of microanatomy of pyramidal neurons and synaptology in the neocortex and hippocampus of rodents and humans) have contributed to this publication.

Publication abstract: *'Secretagogin (SCGN) is a recently discovered calcium-binding protein belonging to the group of EF-hand calcium-binding proteins. SCGN immunostaining has been described in various regions of the human, rat and mouse brain. In these studies, it has been reported that, in general, the patterns of SCGN staining differ between rodents and human brains. These differences have been interpreted as uncovering phylogenetic differences in SCGN expression. Nevertheless, an important aspect that is not usually taken into account is that different methods are used for obtaining and processing brain tissue coming from humans and experimental animals. This is a critical issue since it has been shown that post-mortem time delay and the method of fixation (i.e., perfused vs. nonperfused brains) may influence the results of the immunostaining. Thus, it is not clear whether differences found in comparative studies with the human brain are simply due to technical factors or species-specific differences. In the present study, we analyzed the pattern of SCGN immunostaining in the adult human hippocampal formation (DG, CA1, CA2, CA3, subiculum, presubiculum, and parasubiculum) as well as in the entorhinal and perirhinal cortices. This pattern of immunostaining was compared with rat and mouse that were fixed either by perfusion or immersion and with different post-mortem time delays (up to 5 hr) to mimic the way the human brain tissue is usually processed. We found a number of clear similarities and differences in the pattern of labeling among the human, rat, and mouse in these brain regions as well as between the different brain regions examined within each species. These differences were not due to the fixation'.*

Main highlights:

- We have demonstrated clear differences and similarities in the pattern of secretagogin immunostaining among the human, rat, and mouse in multiple brain regions
- Post-mortem delays of up to 5 hr do not affect the general pattern of secretagogin labeling
- Some patterns of immunostaining were different between the human and either rat or mouse as well as between the two nonhuman species themselves

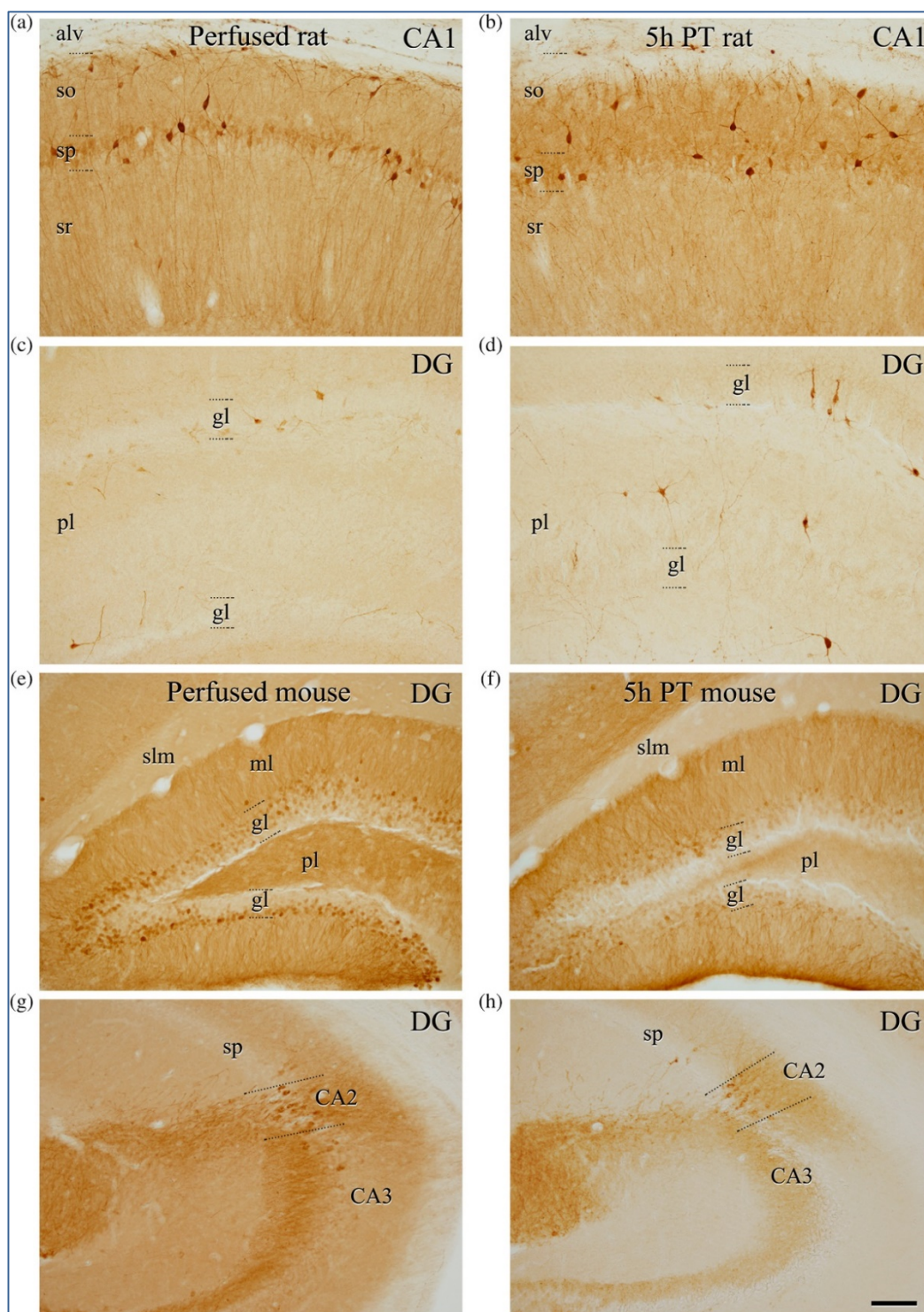


Figure 7: 'Comparison of the patterns of SCGN-immunoreactivity in the hippocampus of the rat and mouse'

'Comparison of the patterns of SCGN-immunoreactivity in the hippocampus of the rat and mouse from brains fixed by perfusion or by immersion. (a-d) Low-magnification photomicrographs showing the distribution patterns of SCGN-immunoreactivity in sections through the CA1 and DG of rat brain fixed by perfusion (a and c) or by immersion after 5 hr PT (b, d). (e-h) Low-magnification photomicrographs showing the distribution patterns of SCGN immunostaining in sections through CA1 and DG of mouse brain fixed by perfusion (e, g) or by immersion after 5 hr PT (f, h). Note the similar pattern of immunostaining obtained for the two experimental conditions (perfused vs. fixed by immersion after 5 hr PT). alv, alveus; CA1, CA1 field of the hippocampus; CA2, CA2 field of the hippocampus; CA3, CA3 field of the hippocampus; DG, dentate gyrus; gl, granular layer; ml, molecular layer; pl, polymorphic layer; slm, stratum lacunosum moleculare; so, stratum oriens; sp, stratum pyramidale; sr, stratum radiatum. Scale bar shown in (h) indicates 90µm in all panels'.

Source: <https://www.ncbi.nlm.nih.gov/pmc/articles/PMC6972606/>

Title: publication title

Publication abstract: taken from the publication

Main highlights: written by the author for this report  
 Figure: example of one figure displayed in the publication

Table 5: Output 5 Links

Component	Link to	URL
C1740, C1741	Data Repository	<a href="https://doi.org/10.1002/cne.24773">https://doi.org/10.1002/cne.24773</a> Images can be downloaded from the publication
	Technical and User documentation	<a href="https://doi.org/10.1002/cne.24773">https://doi.org/10.1002/cne.24773</a>

SPs involved: SP1 - Mouse Brain Organization and Interspecies Comparisons.

Publication reference:

P2147: Differential expression of secretagogin immunostaining in the hippocampal formation and the entorhinal and perirhinal cortices of humans, rats, and mice. Tapia-González S, Insausti R, DeFelipe J. 11 September 2019. <https://doi.org/10.1002/cne.24773>

Documentation, materials, analysis scripts and raw data can be provided upon request from the corresponding author

### 3.1.7 ***Output 6: Calbindin immunostaining in the CA1 hippocampal pyramidal cell layer of the human and mouse: A comparative study***

Data (images) generated for Components C1740 and C1741 (T1.5.1: Comparative studies of microanatomy of pyramidal neurons and synaptology in the neocortex and hippocampus of rodents and humans) have contributed to this publication.

Publication abstract: *'Immunostaining for calbindin (CB) is commonly used to label particular populations of neurons. Recently, it has been shown that the CA1 pyramidal cells in the mouse can be subdivided along the radial axis into superficial and deep pyramidal cells and that this segregation in the radial axis may represent a general principle of structural and functional organization of the hippocampus. One of the most widely used markers of the superficial pyramidal cells is CB. However, this laminar segregation of pyramidal cells has not been reported in the human CA1 using CB immunostaining. The problem is that the different pattern of CB immunostaining observed in the mouse compared to the human could be explained by technical features, of which one of the most important is the postmortem time (PT) delay typical of the brain tissue obtained from humans. In the present study, we have studied the influences of PT delays and fixation procedures and we found that the clear differences found between the CA1 of the human and mouse do not depend on the fixation, but represent actual species-specific differences. These remarkable differences between species should be taken into consideration when making interpretations in translational studies from mouse to human brains'.*

*'Main highlights:*

- *CA1 show different immunostaining pattern for CB in human compared to mouse*
- *Patterns for CB immunostaining do not depend on the fixation of the brain tissue*
- *Species differences should be taken into consideration in translational studies'*

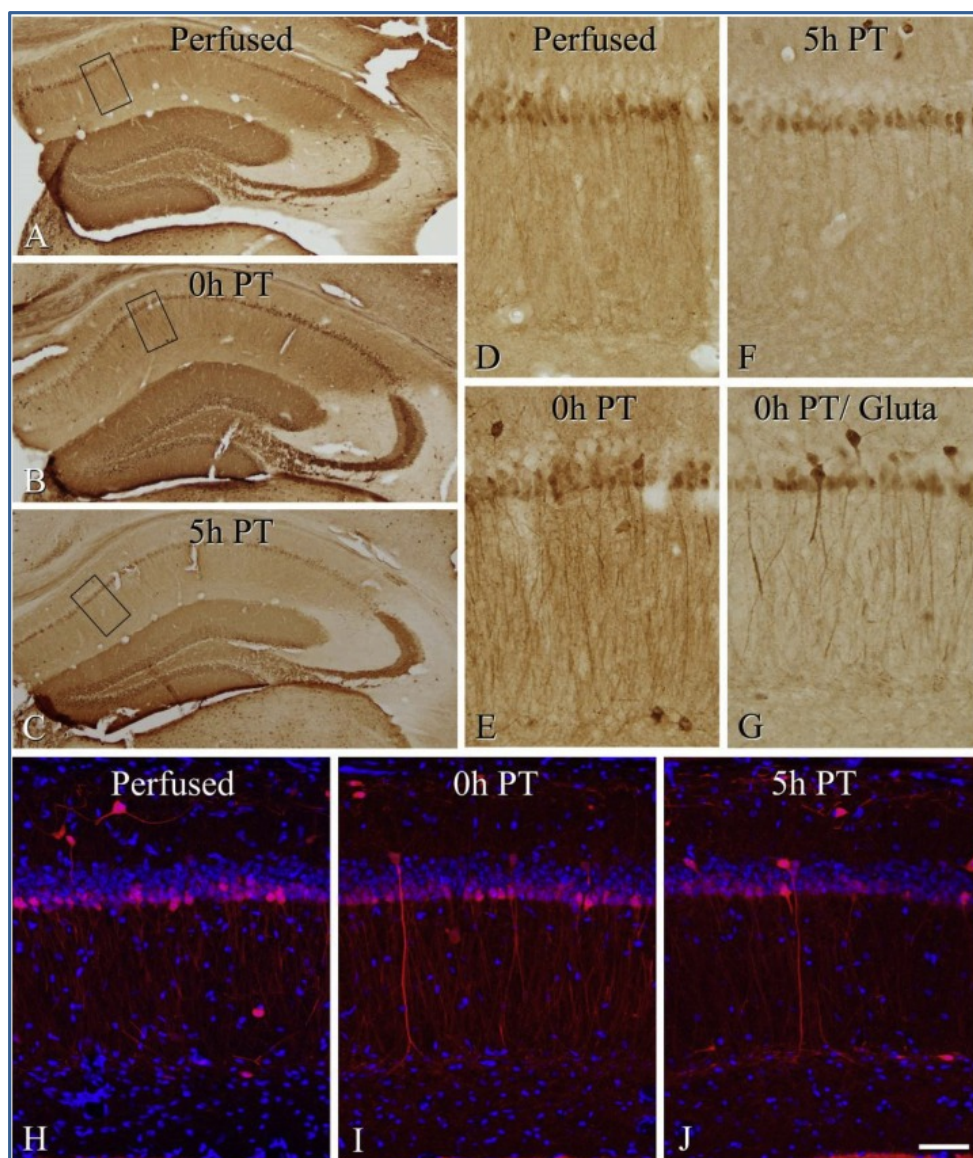


Figure 8: 'CB-ir neurons show sub-laminar distribution in mouse CA1 pyramidal cell layer'

CB immunostaining in mouse hippocampus under different experimental conditions. (A-C) Low-magnification photomicrographs showing CB immunostaining of sections from the hippocampus of a perfused brain (A), or fixed by immersion immediately after death (PT 0 h, 0 min) (B), or by immersion after 5 h PT (C). (D-G) High-magnification photomicrographs to show in greater detail the differences in immunostaining under different experimental conditions. The areas indicated by a rectangle in A, B and C are shown at a higher magnification in D, F and E, respectively. (H-J) Confocal images taken from the pyramidal cell layer of CA1 in sections immunostained for CB and counterstained with DAPI from a perfused mouse brain (H), or fixed by immersion immediately after death (PT 0 h, 0 min) (I), or by immersion after 5 h PT (J). Scale bar shown in J indicates 250  $\mu\text{m}$  in A-C, 43  $\mu\text{m}$  in D-G and 48  $\mu\text{m}$  in H-J.

Source: <https://doi.org/10.1016/j.jchemneu.2020.101745>

Title: publication title

Publication abstract: taken from the publication

Main highlights: taken from the publication

Figure: example of one figure displayed in the publication

Table 6: Output 6 Links

Component	Link to	URL
C1740, C1741	Data Repository	<a href="https://doi.org/10.1016/j.jchemneu.2020.101745">https://doi.org/10.1016/j.jchemneu.2020.101745</a> Images can be downloaded from the publication
	Technical and User documentation	<a href="https://doi.org/10.1016/j.jchemneu.2020.101745">https://doi.org/10.1016/j.jchemneu.2020.101745</a>

SPs involved: SP1 - Mouse Brain Organization and Interspecies Comparisons.

Publication reference:

P2380: Calbindin immunostaining in the CA1 hippocampal pyramidal cell layer of the human and mouse: A comparative study. Merino-Serrais P, Tapia-González S, DeFelipe J. 1 Mar 2020. <https://doi.org/10.1016/j.jchemneu.2020.101745>.

Documentation, materials, data analysis and raw data can be provided upon request from the corresponding author.

### 3.1.8 ***Output 7: Cell Type-Specific Modulation of Layer 6A Excitatory Microcircuits by Acetylcholine in Rat Barrel Cortex***

Data generated for Component C2345 (T1.5.6: Functional characterization of neuromodulator on the single neuron level in motor and sensory cortices of rodent brain) have contributed to this publication.

**Publication abstract:** *'Acetylcholine (ACh) is known to regulate cortical activity during different behavioral states, e.g. wakefulness and attention. Here we show a differential expression of muscarinic ACh receptors (mAChRs) and nicotinic AChRs (nAChRs) in different layer 6A (L6A) pyramidal cell (PC) types of somatosensory cortex. At low concentrations, ACh induced a persistent hyperpolarization in corticocortical (CC) but a depolarization in corticothalamic (CT) L6A PCs via M4 and M1 mAChRs, respectively. At ~1 mM ACh depolarized exclusively CT PCs via  $\alpha$ 4B2 subunit-containing nAChRs without affecting CC PCs. Miniature EPSC frequency in CC PCs was decreased by ACh but increased in CT PCs. In synaptic connections with a presynaptic CC PC, glutamate release was suppressed via M4 mAChR activation but enhanced by nAChRs via  $\alpha$ 4B2 nAChRs when the presynaptic neuron was a CT PC. Thus, in layer 6A the interaction of mAChRs and nAChRs results in an altered excitability and synaptic release, effectively strengthening corticothalamic output while weakening corticocortical synaptic signaling'.*

*'Main highlights:*

- *ACh either depolarizes or hyperpolarizes L6A PCs through activation of mAChRs*
- *Cholinergic responses in L6A PCs are cell-type specific*
- *CT PCs are selectively activated by high concentrations of ACh via  $\alpha$ 4B2 nAChRs*
- *ACh differentially modulate miniature spontaneous activity of CC and CT L6A PCs*
- *ACh induces a reduction of presynaptic neurotransmitter release in CC L6A PCs but an increase in CT PCs'*

Table 7: Output 7 Links

Component	Link to	URL
C2345	Data Repository	<a href="https://doi.org/10.25493/93YQ-6QM">https://doi.org/10.25493/93YQ-6QM</a> <a href="https://doi.org/10.25493/A4RG-CJN">https://doi.org/10.25493/A4RG-CJN</a> <a href="https://doi.org/10.25493/YMV3-45H">https://doi.org/10.25493/YMV3-45H</a>
	Technical and User documentation	In 'Data Descriptor' in the above link and also at <a href="https://www.biorxiv.org/content/biorxiv/early/2019/09/02/701318.full.pdf">https://www.biorxiv.org/content/biorxiv/early/2019/09/02/701318.full.pdf</a>

SPs involved: SP1 - Mouse Brain Organization and Interspecies Comparisons; SP2 - Human Brain Organization.

Publication reference:

P2118: Cell Type-Specific Modulation of Layer 6A Excitatory Microcircuits by Acetylcholine in Rat Barrel Cortex. Yang D, Günter R, Qi G, Radnikow G, Feldmeyer D. 14 July 2019. DOI: 10.1101/701318.

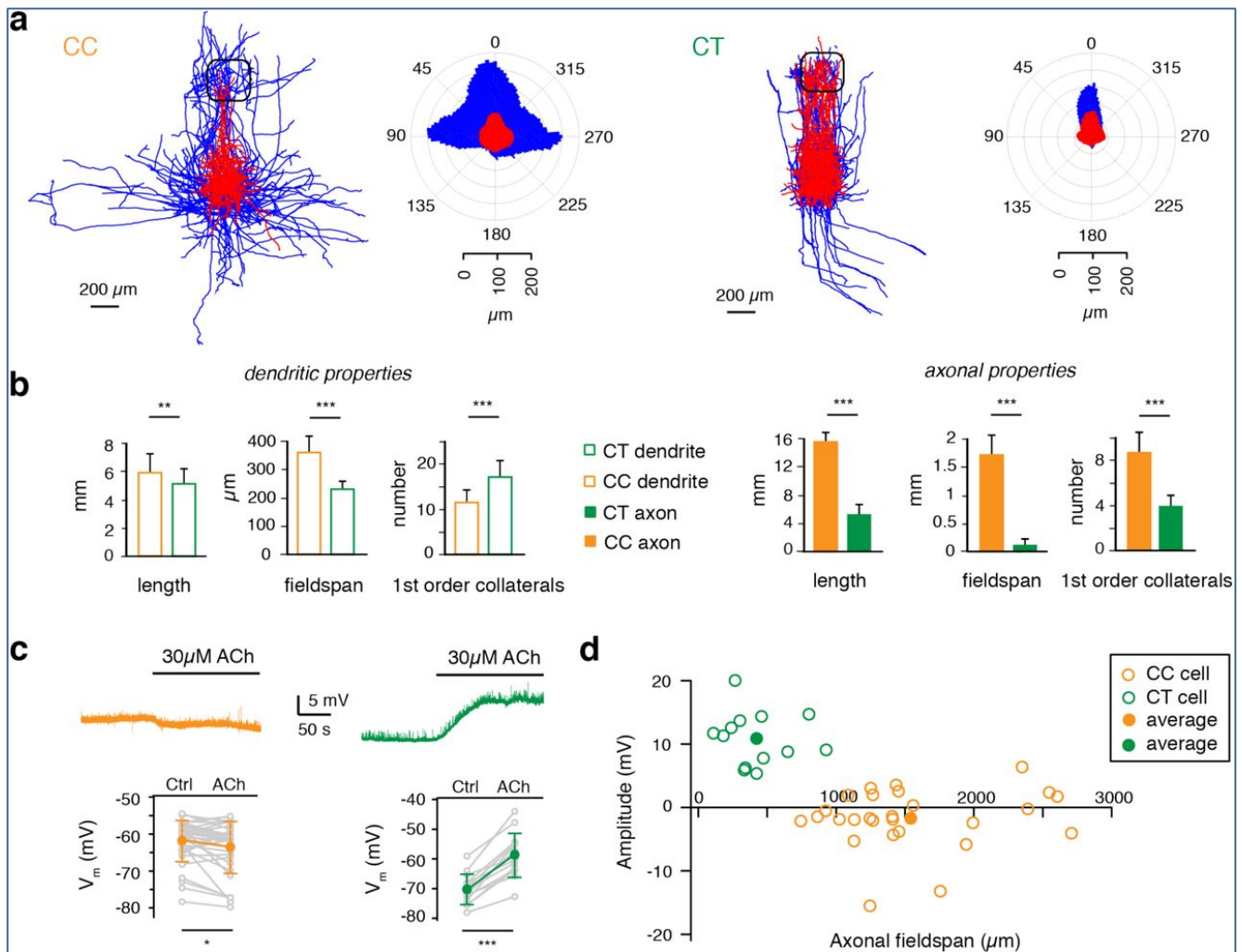


**Figure 9: 'ACh hyperpolarizes CC L6A PCs but depolarizes CT L6A PCs'**

'(a) Left, overlay of reconstructions of CC and CT PCs. Reconstructions of PCs were aligned with respect to the barrel center. Right, polar plots of CC and CT PCs.  $n = 15$  for each group. Somatodendrites are shown in red and axons are shown in blue. (b) Histograms comparing the length, fieldspan and number of first order collaterals of axonal and dendritic structures for the two groups of PCs.  $n = 21$  for CC neurons and  $n = 54$  for CT neurons. Dendritic length:  $p = 0.0015$ , dendritic fieldspan:  $p = 1.4 \times 10^{-10}$ , number of dendritic main nodes:  $p = 1.7 \times 10^{-6}$ ; Axonal length:  $p = 9.6 \times 10^{-8}$ , dendritic fieldspan:  $p = 4.8 \times 10^{-11}$ , number of axonal main nodes:  $p = 8.5 \times 10^{-11}$  for Mann-Whitney U-test. (c) Top, representative current-clamp recordings of a depolarizing CC (orange) and a hyperpolarizing CT pyramidal cell (green) following bath application of 30 $\mu$ M ACh. Bottom, histograms of resting membrane potential ( $V_m$ ) of L6A CC PCs in control and in the presence of 30  $\mu$ M ACh ( $n = 35$ ,  $p = 0.019$  for Wilcoxon signed-rank test) and CT ( $n = 14$ ,  $p = 6.1 \times 10^{-5}$  for Wilcoxon signed-rank test) PCs. (d) Plots of the ACh-induced change in  $V_m$  vs axonal fieldspan for two subtypes of PCs. Open orange circles, data from individual CC PCs ( $n = 27$ ); open green circles, data from individual CT PCs ( $n = 13$ ). Filled orange circle, average data from CC cells; filled green circle, average data from CT cells'.

Source: <https://doi.org/10.1101/701318>

Title: publication title

Publication abstract: taken from the publication

Main highlights: taken from the section 'Results' of publication

Figure: example of one figure displayed in the publication

### 3.1.9 Output 8: Comparing basal dendrite branches in human and mouse hippocampal CA1 pyramidal neurons with Bayesian networks

Data generated for Component C1740 (T1.5.1: Comparative studies of microanatomy of pyramidal neurons and synaptology in the neocortex and hippocampus of rodents and humans) have contributed

to this publication. T1.5.5: Machine learning-based comparative studies of microanatomy and physiology of mice and humans (C1802, C1803, and C1804) has also contributed to this Output.

**Publication abstract:** *'Pyramidal neurons are the most common cell type in the cerebral cortex. Understanding how they differ between species is a key challenge in neuroscience. A recent study provided a unique set of human and mouse pyramidal neurons of the CA1 region of the hippocampus, and used it to compare the morphology of apical and basal dendritic branches of the two species. The study found inter-species differences in the magnitude of the morphometrics and similarities regarding their variation with respect to morphological determinants such as branch type and branch order. We use the same data set to perform additional comparisons of basal dendrites. In order to isolate the heterogeneity due to intrinsic differences between species from the heterogeneity due to differences in morphological determinants, we fit multivariate models over the morphometrics and the determinants. In particular, we use conditional linear Gaussian Bayesian networks, which provide a concise graphical representation of the independencies and correlations among the variables. We also extend the previous study by considering additional morphometrics and by formally testing test whether a morphometric increases or decreases with the distance from the soma. This study introduces a multivariate methodology for inter-species comparison of morphology'.*

**'Main highlights:**

- This study is an example on how to use data generated in SP1 to develop statistical models
- Bayesian networks are introduced as a multivariate model for comparison between species
- Bayesian networks are faithful models of the branch-level morphologies between species
- Bayesian networks could be used for more purposes than comparison, such as to generate synthetic branches or to perform probabilistic queries about the morphology'

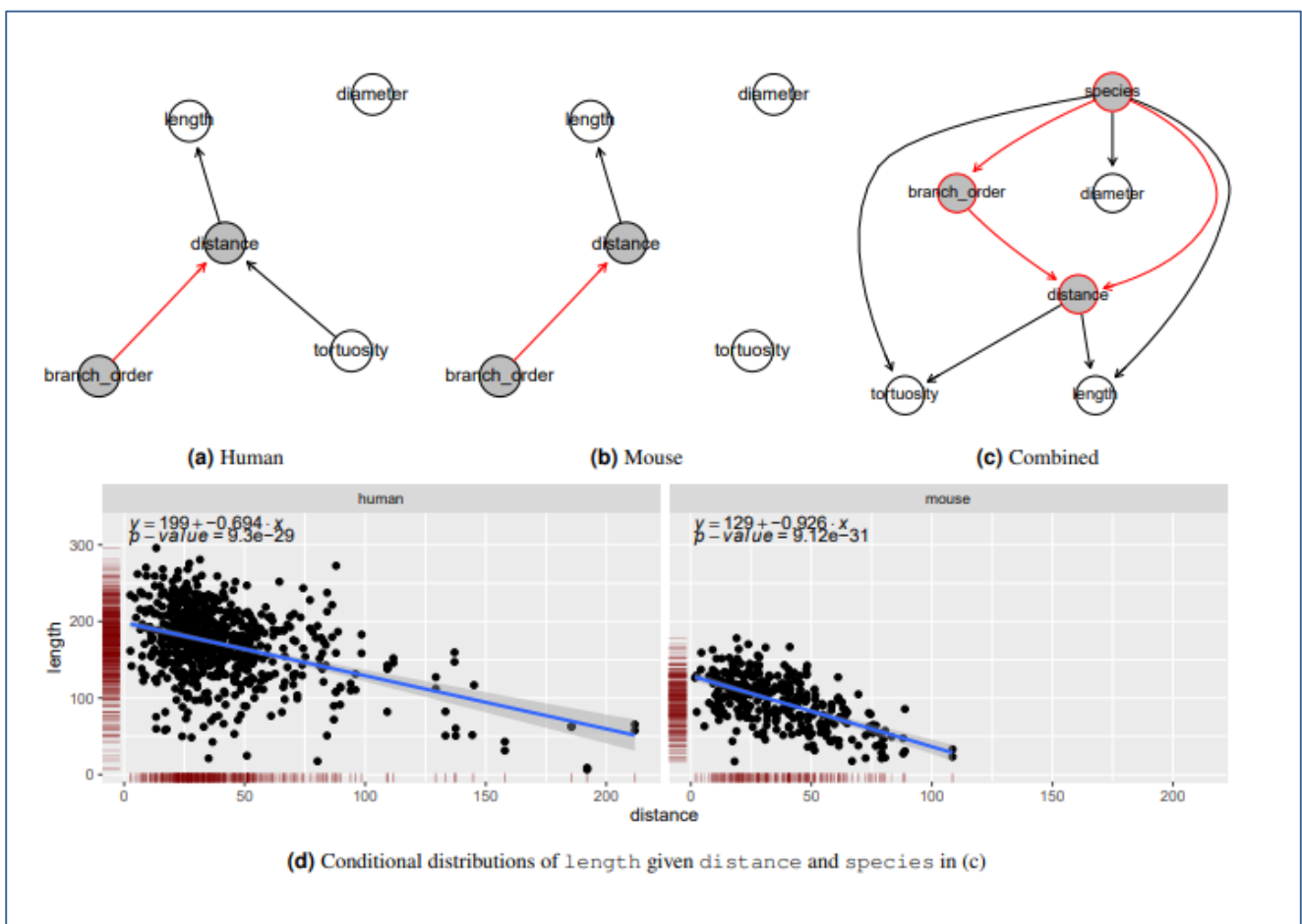


Figure 10: 'Bayesian networks learned from the terminal branches'

'Human data (a), mouse data (b), and data of both species (c). Proximity between two nodes of a graph is unrelated to the strength of their correlation. The nodes of the morphological determinants are shaded in grey with red

borders. Arcs among morphological determinants are depicted in red. (d) Scatter plots depicting the conditional distribution of length on distance, for the human (left) and for the mouse (right). The linear regression line shows the mean of the fitted conditional distribution of length as a function of distance, with its formula given in the top part of the panel, with  $y$  standing for length and  $x$  for distance. The band shows a 95% confidence interval around the mean'.

Source: <https://www.biorxiv.org/content/10.1101/2020.03.14.991828v1>

Title: publication title

Publication abstract: taken from the publication

Main highlights: taken from the section 'Results' of publication and written by the author for this report

Figure: example of one figure displayed in the publication

Table 8: Output 8 Links

Component	Link to	URL
C1740	Data Repository	<a href="https://kg.ebrains.eu/search/instances/Dataset/2d3757b5-afc8-470d-988e-f382884cf382">https://kg.ebrains.eu/search/instances/Dataset/2d3757b5-afc8-470d-988e-f382884cf382</a> (embargoed); DOI: 10.25493/H24F-2ET
	Technical and User documentation	Data descriptor in the KG
C1802	Model Repository	<a href="https://kg.ebrains.eu/search/instances/Model/5ae92dbb-cb01-45be-9eaa-400b54921602">https://kg.ebrains.eu/search/instances/Model/5ae92dbb-cb01-45be-9eaa-400b54921602</a>
	Technical and User documentation	In the above link and also at <a href="https://www.biorxiv.org/content/10.1101/2020.03.14.991828v1">https://www.biorxiv.org/content/10.1101/2020.03.14.991828v1</a>

SPs involved: SP1 - Mouse Brain Organization and Interspecies Comparisons

Publication reference:

P2428: Comparing basal dendrite branches in human and mouse hippocampal CA1 pyramidal neurons with Bayesian networks. Mihaljevic B, P. Larrañaga P, Benavides-Piccione R, DeFelipe J, and Bielza C. 2020. Preprint DOI: <https://doi.org/10.1101/2020.03.14.991828>

Other related publications are as follows:

P1722: Towards a supervised classification of neocortical interneuron morphologies. Mihaljević B, Larrañaga P, Benavides-Piccione R, Hill S, DeFelipe J, Concha Bielza C. 1 December 2018. DOI: [10.1186/s12859-018-2470-1](https://doi.org/10.1186/s12859-018-2470-1)

P1723: Patterns of dendritic basal field orientation of pyramidal neurons in the rat somatosensory cortex. Leguey I, Benavides-Piccione R, Rojo C, Larrañaga P, Bielza C, DeFelipe J. 17 December 2018 DOI: 10.1523/ENEURO.0142-18.2018. <https://www.ncbi.nlm.nih.gov/pmc/articles/PMC6335082/>

P1724: A regularity index for dendrites - local statistics of a neuron's input space. Anton-Sanchez, Effenberger F, Bielza C, Larrañaga P, Cuntz H. 12 November 2018. DOI: [10.1371/journal.pcbi.1006593](https://doi.org/10.1371/journal.pcbi.1006593)

P1821: Tractable learning of Bayesian networks from partially observed data. Marco Benjumbeda, Sergio Luengo-Sanchez, Pedro Larrañaga, Concha Bielza. 2019. Pattern Recognition, Vol. 91. [http://dx.doi.org/10.1016/j.patcog.2019.02.025](https://doi.org/10.1016/j.patcog.2019.02.025)

P2138: Classification of GABAergic interneurons by leading neuroscientists. Mihaljevic B, Benavides-Piccione R, Bielza C, P. Larrañaga P, and DeFelipe J, Scientific Data, 22 October 2019. DOI: [10.6084/m9.figshare.9948803](https://doi.org/10.6084/m9.figshare.9948803).

### 3.1.10 Others

Other outputs achieved in SP1 during the SGA2 that can contribute to the implementation of the comparative studies are as follows:

- Output 1 (3D reconstruction, measurements and registration to cortical areal maps of the individual morphology of thalamic projection neurons from motor and sensory relay thalamic nuclei, C1867) contributing to KR1.2: High-level multiscale datasets at cellular and microcircuit level on selected brain regions: neocortex (including thalamus), hippocampus, basal ganglia and cerebellum and KR1.4: Multi-level datasets generated by integrating neuroanatomical data with

genetic, molecular and physiological data using advanced technologies from SGA2 Deliverable D1.6.2 (Section 4.1)

- Output 7 (*Integrated framework for the interactive exploratory analysis of neurological data, C1870*) contributing to KR1.4 from SGA2 Deliverable D1.6.2 (Section 6.1)

The detailed description of these Outputs can be found in the deliverable mentioned above.

## 3.2 Validation and Impact

### 3.2.1 *Actual and Potential Use of Output(s)*

Outputs 1, 2 and 3: These Outputs reveal new differences on the physiology of mouse and human neocortical excitatory synapses as well as of neuromodulation of neocortical circuits in mouse and human brains. They are validated by peer-review publications. The impact registered of this publication is as follows: Output 1: Article accesses: 2627; Citations: 9 (<https://www.nature.com/articles/s41467-018-06628-w/metrics>; last updated: Mon, 2 Mar 2020); Output 2: total views: 1412 (1169 views and 243 downloads) (<http://loop-impact.frontiersin.org/impact/article/469926#totalviews/views>; last updated: Mon, 2 Mar 2020); Output 3: Article accesses: 1691; <https://www.nature.com/articles/s41467-019-13244-9/metrics>; last update Wed, 11 Mar 2020).

- Output 1: Lateral inhibition by Martinotti interneurons is facilitated by cholinergic inputs in human and mouse neocortex (P1410)

Inhibition of pyramidal neurons by GABAergic interneurons is essential for cortical computation. Several circuit motifs have been identified by which interneurons shape cortical signal propagation, among which are feedforward inhibition, feedback inhibition and disinhibition. In each of these motifs, several distinct types of interneurons can be involved. Because of the profound difference in projection targets on pyramidal neuron dendrites between PV and SOM axons, whereby PV neurons innervate perisomatic regions and SOM neurons generally target distal dendrites, lateral inhibition by PV neurons may be more involved in rapidly silencing action potential firing in neighboring pyramidal neurons, while lateral inhibition through SOM neurons will control synaptic integration, burst firing and dendritic regenerative phenomena. What the precise impact will be of lateral inhibition by a given interneuron type at any point in time will depend among other things on neuromodulatory conditions, but this is poorly understood. Both PV and SOM interneurons are modulated by various neurotransmitters and in particular SOM interneurons are strongly modulated by acetylcholine. The cortex receives cholinergic inputs mainly from the basal forebrain. How cholinergic inputs affect lateral inhibition is not known. It is also not known whether lateral inhibition between pyramidal neurons exists in human neocortical circuits. These issues are resolved in this paper.

- Output 2: Group I mGluR-Mediated Activation of Martinotti Cells Inhibits Local Cortical Circuitry in Human Cortex (P1962)

Group I metabotropic glutamate receptors (mGluRs) mediate a range of signalling and plasticity processes in the brain and are of growing importance as potential therapeutic targets in clinical trials for neuropsychiatric and neurodevelopmental disorders (NDDs). Fundamental knowledge regarding the functional effects of mGluRs upon pyramidal neurons and interneurons is derived largely from rodent brain, and their effects upon human neurons are predominantly untested. We therefore addressed how group I mGluRs affect microcircuits in human neocortex. We show that activation of group I mGluRs elicits action potential firing in Martinotti cells, which leads to increased synaptic inhibition onto neighboring neurons. Some other interneurons, including fast-spiking interneurons, are depolarized but do not fire action potentials in response to group I mGluR activation. Furthermore, we confirm the existence of group I mGluR-mediated depression of excitatory synapses in human pyramidal neurons. We propose that the strong increase in inhibition and depression of excitatory synapses onto layer 2/3 pyramidal neurons upon group I mGluR activation likely results in a shift in the balance between excitation and inhibition in the human cortical network.

In recent years, group I mGluRs, have become of increasing interest as potential therapeutic targets in neuropsychiatric and neurodevelopmental disorders (NDDs), including schizophrenia, and autistic spectrum disorders (ASDs). Unfortunately, clinical trials have thus far been unsuccessful, with reasons given ranging from patient age, and drug dosage level, to incomplete knowledge at a brain circuit rather than at a single cell level. Furthermore, rodent data on mGluR function has rarely been validated in the human brain. This paper shows how human neocortical circuits are modulated by group 1 mGluRs.

- Output 3: Prefrontal cortical ChAT-VIP interneurons provide local excitation by cholinergic synaptic transmission and control attention (P2212)

This paper shows that in the rodent neocortex, the neuromodulator acetylcholine (ACh) is produced intrinsically in neocortical ChAT-VIP neurons that directly excite neighbouring neurons in several layers through fast synaptic transmission of ACh. Both interneurons in layers (L) 1-3 as well as pyramidal neurons in L2/3 and L6 receive direct inputs from ChAT-VIP neurons mediated by fast cholinergic transmission. A fraction (10-20%) of postsynaptic neurons that received cholinergic input from ChAT-VIP interneurons also received GABAergic input from these neurons. In contrast to regular VIP interneurons, ChAT-VIP neurons did not disinhibit pyramidal neurons. Finally, we show that activity of these neurons is relevant for behaviour and they control attention behaviour distinctly from basal forebrain ACh inputs. Thus, ChAT-VIP neurons are a local source of cortical ACh that directly excite neurons throughout cortical layers and contribute to attention. These neurons do not exist in human neocortex, and therefore highlight a marked difference in cortical processing mechanisms between human and rodent.

Data from these outputs have also been used to build single cell neocortical models. These models are published in the KG are as follows:

Active Model of Human Cortical Pyramidal Neurons in Layer 2/3 - Cell 5/1503  
[https://kg.ebrains.eu/search/?facet\\_type\[0\]=Model&facet\\_Model\\_brainStructures\[0\]=cerebral%20cortex&p=2#Model/a335f3c3ef3da4c83646543a633dda25](https://kg.ebrains.eu/search/?facet_type[0]=Model&facet_Model_brainStructures[0]=cerebral%20cortex&p=2#Model/a335f3c3ef3da4c83646543a633dda25))

Passive Model of Human Cortical Pyramidal Neurons in Layer 2/3 - Cell 3/0603  
[https://kg.ebrains.eu/search/?facet\\_type\[0\]=Model&facet\\_Model\\_brainStructures\[0\]=cerebral%20cortex#Model/8fe71cbe0972a0b4720e4ab71f49a6c1](https://kg.ebrains.eu/search/?facet_type[0]=Model&facet_Model_brainStructures[0]=cerebral%20cortex#Model/8fe71cbe0972a0b4720e4ab71f49a6c1))

Active Model of Human Cortical Pyramidal Neurons in Layer 2/3 - Cell 3/1303  
<https://kg.ebrains.eu/search/instances/Model/936e8a85737ff64db07a1846148fe006>)

Active Model of Human Cortical Pyramidal Neurons in Layer 2/3 - Cell 3/0603  
[https://kg.ebrains.eu/search/?facet\\_type\[0\]=Model&facet\\_Model\\_brainStructures\[0\]=cerebral%20cortex#Model/f4e09ee31d2547fdd10612c13449e173](https://kg.ebrains.eu/search/?facet_type[0]=Model&facet_Model_brainStructures[0]=cerebral%20cortex#Model/f4e09ee31d2547fdd10612c13449e173))

Active Model of Human Cortical Pyramidal Neurons in Layer 2/3 - Cell 6/1303  
[https://kg.ebrains.eu/search/?facet\\_type\[0\]=Model&facet\\_Model\\_brainStructures\[0\]=cerebral%20cortex#Model/a9da7b5d467a82914f663286a33f992f](https://kg.ebrains.eu/search/?facet_type[0]=Model&facet_Model_brainStructures[0]=cerebral%20cortex#Model/a9da7b5d467a82914f663286a33f992f))

Active Model of Human Cortical Pyramidal Neurons in Layer 2/3 - Cell 8/0603  
[https://kg.ebrains.eu/search/?facet\\_type\[0\]=Model&facet\\_Model\\_brainStructures\[0\]=cerebral%20cortex#Model/5a3ef67be32eaaad45dcf7bf3e545680](https://kg.ebrains.eu/search/?facet_type[0]=Model&facet_Model_brainStructures[0]=cerebral%20cortex#Model/5a3ef67be32eaaad45dcf7bf3e545680))

Active Model of Human Cortical Pyramidal Neurons in Layer 2/3 - Cell 11/0603  
[https://kg.ebrains.eu/search/?facet\\_type\[0\]=Model&facet\\_Model\\_brainStructures\[0\]=cerebral%20cortex#Model/ce74b544925a93f9bcff1b58698ffafe](https://kg.ebrains.eu/search/?facet_type[0]=Model&facet_Model_brainStructures[0]=cerebral%20cortex#Model/ce74b544925a93f9bcff1b58698ffafe))

Output 4: Differential structure of hippocampal CA1 pyramidal neurons in the human and mouse (P1963)

This Output reveals new differences between rodents and human of some morphological parameters of the pyramidal cells. It is validated by a peer-review publication. This Output could be used in comparative modelling of pyramidal neurons in different cortical areas. The impact registered of this publication is as follows: total views: 1474 (1069 page views and 405 downloads) <https://academic.oup.com/cercor/advance-article/doi/10.1093/cercor/bhz122/5527134>; last updated: Mon, 2 Mar 2020).

Output 5: Differential expression of secretogin immunostaining in the hippocampal formation and the entorhinal and perirhinal cortices of humans, rats, and mice (P2147) and Output 6: Calbindin immunostaining in the CA1 hippocampal pyramidal cell layer of the human and mouse: A comparative study (P2380)

These Outputs provide remarkable differences in the expression of particular proteins in brain neurons between species. These differences should be taken into consideration when making interpretations in translational studies from mouse to human brains. They are validated by peer-review publications. The impact will be updated shortly due to the recent publication date. These publications have used data generated in components C1740 (<https://doi.org/10.25493/H24F-2ET>) and C1741 (<https://doi.org/10.25493/PJG9-ZE6>) from Output 4.

Output 7: Cell Type-Specific Modulation of Layer 6A Excitatory Microcircuits by Acetylcholine in Rat Barrel Cortex (P2118)

This Output provides strategic data to implement comparative studies between rodents and human regarding the effects of acetylcholine. How the cortex decides to send strong output to one target region, while sending little to another is poorly understood. This study shows that in output layer 6A, this can be regulated by the neuromodulator ACh. The interaction of mAChRs and nAChRs results in an altered excitability and synaptic release, effectively strengthening corticothalamic output while weakening corticocortical synaptic signalling. The datasets have been validated by a peer-review publication. These data have been generated as the contribution of the task, Functional characterization of neuromodulator on the single neuron level in motor and sensory cortices of rodent brain, T1.5.6 and T2.5.8, in SP1 and SP2, respectively.

Output 8: Comparing basal dendrite branches in human and mouse hippocampal CA1 pyramidal neurons with Bayesian networks (P2428)

A novel way for multivariate comparison and analysis of neuron morphology and electro-physiology data has been introduced. The groundwork for such comparisons has been laid by defining useful metrics, such as the dendritic branching regularity index (P1724), and the NeuroSTR software (<https://computationalintelligencegroup.github.io/neurostr/>) to compute them (e.g., P1722), and the use of circular statistics to analyse dendritic field orientation (P1723).

This Output introduces novel methodology for multivariate comparison and analysis of neuron morphology and electro-physiology data, by analysing compact descriptions of the probability distributions over the morphological and/or electro-physiological features. The paper has been submitted on the morphological comparison between basal dendrites of hippocampus CA1 cells to the open access Scientific Reports journal bioArxiv: DOI 10.1101/2020.03.14.991828. The model has already been shared with the Curation Team to be integrated in the KG. The input to this work are hippocampus cells' data that have been generated within KR1.5 by T1.5.1 (C1740: Comparison of morphological parameters of pyramidal neurons between rodents and humans). Two more papers on the electro-physiology and joint morphology and electro-physiology study and on the comparison of spatial distribution of synapses are in preparation.

### 3.2.2 Publications

Main Outputs outlined in this report are SP1 publications. See Section 3.1.1 for the full list of Outputs. The significance of each publication within the HBP and outside is described above.

Publications that are used in the report are under [open access licenses](#) (Creative Commons Attribution 4.0 International License, Creative Commons CC-BY-NC, Attribution-Non Commercial-No Derivatives 4.0 International (CC BY-NC-ND 4.0); Preprints: copyright holder for preprint is the author/funder. Publications have been used according to them and no changes have been made.

## 4. Conclusion and Outlook

As stated in the DoA, understanding the human brain is extremely challenging – not only because of its complexity and the technical difficulties involved, but also because ethical limitations do not allow all of the necessary datasets to be acquired directly from human brains. The problem is that data from non-human brains cannot fully substitute information on humans since there are fundamental structural and behavioural aspects that are unique to humans as well as to any other species. Accordingly, the question remains as to how much of this non-human brain information can be reliably extrapolated to humans, and indeed it is important to establish what the best strategy currently is for obtaining the missing data. Thus, it is critical to determine the differences and similarities in brain organisation.

The SP1 Objective, SO1.5 ‘Obtaining critical information about differences and similarities in brain organisation across species’, aims to work towards this goal through KR1.5: *Key datasets on single neurons and circuits to be used in comparative studies on human and rodent for modelling. Ground-breaking techniques will be used to generate anatomical and functional datasets. New statistical models will be developed to perform comparative analysis.* Final datasets and models planned in the SGA2 to carry out the comparative studies have been released to contribute to this KR. These Outputs include the final datasets on quantitative data of the neuropil at the ultrastructural level; quantitative ultrastructural data of the mouse hippocampus; as well as 3D reconstructions and functional data of human neocortical pyramidal cells. These new datasets have been used to carry out the comparative studies outlined in this report. Also, novel methodologies for multivariate comparison and analysis of anatomical and functional data have been developed to implement comparative studies.

These Outputs provide crucial information about differences and similarities in brain organisation across species. The similarities between the human, rat and mouse –in terms of the microanatomy and physiology of pyramidal cells and synapses– might be considered as basic bricks of cortical organisation, building a bridge toward the SP2 analysis of the human brain at the integrative level. By contrast, the differences may indicate evolutionary adaptations of cells and synapses to particular functions.

Finally, as mentioned above, the strategic comparative data displayed in this Deliverable are being fed directly into theory and model simulations in SP4 and SP6. Thereby, this KR provides anchor points for translation from rodent neuronal circuit simulations to human neuronal circuit simulations. The data generated in this Deliverable are critical for the transition of the scientific objectives from SGA2 to SGA3, in particular for WP1: *The Human Multiscale Brain Connectome and its Variability* that will be focused on the human brain.

## 5. Annex 1: SP1 Components

The Components contributing to this Deliverable are listed below:

Component ID	Name of the component	Type	Related to WPs	M24 Release
C1729	Comparative physiology of mouse and human neocortical excitatory synapses	Dataset	WP1.5	Functional properties of human excitatory synapses
C1730	Comparative physiology of mouse and human neocortical pyramidal neurons and interneurons	Dataset	WP1.5	Biophysical properties of pyramidal neurons and interneurons in human neocortex: e-codes and reconstructions of pyramidal neurons and interneurons in human temporal neocortex
C1731	Comparative physiology of neuromodulation of neocortical circuits in mouse and human brain	Dataset	WP1.5	Role of attentional modulation on S1HL activity
C1740	Comparison of morphological parameters of pyramidal neurons between rodents and humans	Dataset	WP1.5	Dendritic spines of human and mouse pyramidal cells
C1741	Comparison of morphological parameters of pyramidal neurons between rodents and humans	Dataset	WP1.5	Dendritic spines of human pyramidal cells
C2345	Quantitative analysis of neuromodular function in the rodent neocortex	Dataset	WP1.5	Preliminary data on neuromodulator subtypes
C1802	Principal cells morphology comparative models	Model	WP1.5	Final release of the model
C1870	Integrated environment for acquisition and early analysis of microanatomical data (components merged id: 1870 & id: 1871)	Software	WP1.4, WP1.5	Integrated Environment
C1867	Single-cell 3D reconstruction and measurement of thalamocortical ventral lateral, ventral anterior and parafascicular nuclei	Dataset	WP1.2, WP1.4, WP1.5	Optical microscopy 3D reconstruction and measurement of individually labelled motor thalamocortical cells (final release M24)